DOI: 10.1002/ejic.200900680

Divanadium(V) and Trapped Valence Linear Tetravanadium(IV,V,V,IV) Complexes

Anindita Sarkar[a] and Samudranil Pal*[a]

Keywords: Vanadium / Mixed-valent compounds / EPR spectroscopy / Redox chemistry / Localized valence

In an acetonitrile/water mixture, reactions of the *N*,*N*′-bis(diacetyl)hydrazine (H_2diah), bis(acetylacetonato)oxidovanadium(IV) [$VO(acac)_2$] and monodentate *N*-coordinating heterocycles (hc) in a 1:2:2 mol ratio provide yellow divanadium(V) complexes of formula [$(hc)O_2V(\mu$-diah)$VO_2(hc)$] (**1**, hc = imidazole; **2**, hc = pyrazole; **3**, hc = 3,5-dimethyl pyrazole). On the other hand, in the same solvent mixture reactions of the same reagents in a 1:4:2 mol ratio produce green linear tetravanadium(IV,V,V,IV) complexes of formula [$(acac)_2OV(\mu$-O)VO(hc)(μ-diah)(hc)OV(μ-O)VO$(acac)_2$] (**4**, hc = imidazole; **5**, hc = pyrazole; **6**, hc = 3,5-dimethyl pyrazole). The complexes **1**–**6** have been characterized by elemental analysis, magnetic susceptibility, and various spectroscopic and electrochemical measurements. The X-ray crystal structures of **1**, **3** and **6** have been determined. In all three structures, the diazine ligand $diah^{2-}$ is in *trans* configuration. Metal-centred bond parameters are consistent with the localized electronic structure of the two *trans*-bent $\{OV(\mu\text{-}O)VO\}^{3+}$ cores present in **6**. The pentavalent metal centres in **1**, **3** and **6** are in a distorted trigonal-bipyramidal N_2O_3 coordination environment, while the terminal tetravalent metal centres in **6** are in a distorted octahedral O_6 coordination sphere. The eight-line EPR spectra of the tetravanadium species (**4**–**6**) in dimethyl sulfoxide at ambient temperature indicate the rare valence localized electronic structure in the fluid phase. All the complexes are redox active and display metal-centred electron transfer processes in dimethyl sulfoxide solution. A reduction within –0.78 to –0.94 V (vs. Ag/AgCl) is observed for the divanadium(V) species **1**–**3**, while a reduction and an oxidation are observed in the potential ranges –0.82 to –0.90 V and 0.96 to 1.12 V (vs. Ag/AgCl), respectively, for the tetravanadium species **4**–**6**.
(© Wiley-VCH Verlag GmbH & Co. KGaA, 69451 Weinheim, Germany, 2009)

Introduction

The chemistry of multinuclear oxido-bridged vanadium complexes has been a subject of continuous interest over the past two decades because of the biochemical importance of these species and their potential use as therapeutic agents and oxidation catalysts.[1] We have been working on oxidovanadium(IV/V) complexes with acid hydrazide based Schiff bases for some time.[2] Recently we reported a coordinatively unsymmetrical complex (variation in the ligands bonded to the two metal centres) of the mixed valence *syn*-$\{OV(\mu\text{-}O)VO\}^{3+}$ core that is of trapped valence character in the solid state as well as in solution at ambient temperature.[2h] Before this, there was a solitary report on a complex with the same core, where the two tridentate ligands attached to the two metal centres differ only in the substituent on the aromatic fragment,[3l] and there were very few examples of the $\{OV(\mu\text{-}O)VO\}^{3+}$ with a valence localized electronic structure in the fluid state.[3g,3i,3l] Compared to dinuclear species, tetranuclear complexes composed of two $\{OV(\mu\text{-}O)VO\}^{3+}$ units are extremely rare. To the best of our knowledge only three structurally characterized complexes of this type are known (Scheme 1).[4] Each of these species has a pair of dinucleating ligands. The dinucleating ligand contains two tripodal ends connected by a spacer having one or two additional coordinating sites. The tripodal ends of each ligand bind two $\{OV(\mu\text{-}O)VO\}^{3+}$ units and as a result these complexes have cyclic structures. In one of these three complexes the metal centres of the $\{OV(\mu\text{-}O)VO\}^{3+}$ cores are coordinatively unsymmetrical[4b] and in the remaining two complexes they are symmetrical (Scheme 1).[4a,4c] All these complexes are trapped valence in the solid state. However, EPR studies of only one of them are reported and the complex has valence delocalized electronic structure in solution at ambient temperature.[4b]

In the present work, we report a series of dinuclear dioxidovanadium(V) complexes, [$(hc)O_2V(\mu$-diah)$VO_2(hc)$], with the deprotonated O,N,NO-donor *N*,*N*′-bis(diacetyl)-hydrazine ($diah^{2-}$) as the bridging ligand and neutral monodentate N-donor heterocycles (hc) as ancillary ligands and the linear tetravanadium(IV,V,V,IV) complexes, [$(acac)_2OV(\mu$-O)VO(hc)(μ-diah)(hc)OV(μ-O)VO$(acac)_2$], containing two unsymmetrical $\{OV(\mu\text{-}O)VO\}^{3+}$ units formed by the attachment of two [$VO(acac)_2$] ($acac^-$ = acetylacetonate) molecules at the two ends of the dinuclear species (Scheme 1). The electronic structure of the coordinatively unsymmetrical $\{OV(\mu\text{-}O)VO\}^{3+}$ units in the tetravanadium species has been scrutinized. Molecular structures of repre-

[a] School of Chemistry, University of Hyderabad, Hyderabad 500 046, India
E-mail: spsc@uohyd.ernet.in

 © 2009 Wiley-VCH Verlag GmbH & Co. KGaA, Weinheim

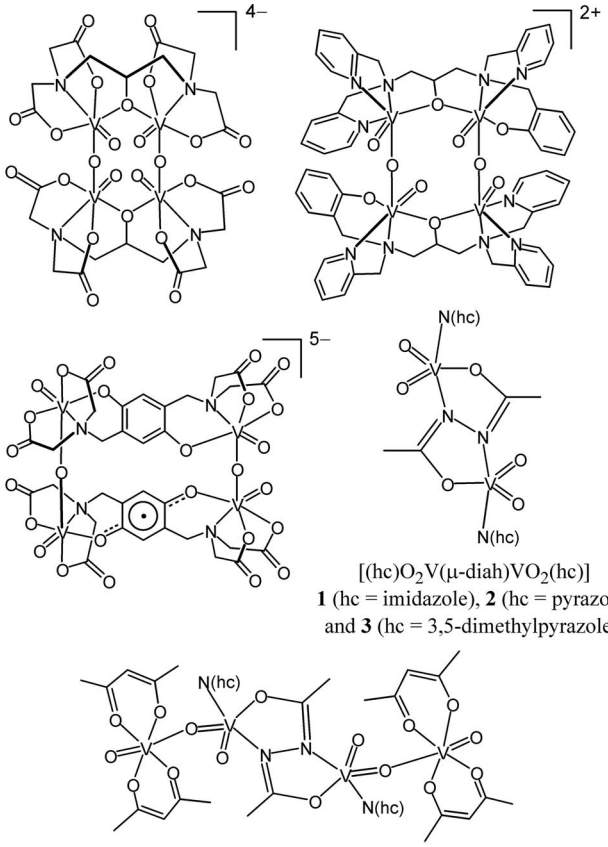

$[(hc)O_2V(\mu\text{-diah})VO_2(hc)]$
1 (hc = imidazole), **2** (hc = pyrazole)
and **3** (hc = 3,5-dimethylpyrazole)

$[(acac)_2OV(\mu\text{-O})VO(hc)(\mu\text{-diah})(hc)OV(\mu\text{-O})VO(acac)_2]$
4 (hc = imidazole), **5** (hc = pyrazole) and **6** (hc = 3,5-dimethylpyrazole)

Scheme 1. Previously reported cyclic tetravanadium complexes containing two $\{OV(\mu\text{-O})VO\}^{3+}$ units and the complexes reported in the present work.

sentative dinuclear dioxidovanadium(V) and tetravanadium(IV,V,V,IV) complexes have been confirmed by single-crystal X-ray diffraction analysis.

Results and Discussion

Syntheses

The divanadium(V) complexes, $[(hc)O_2V(\mu\text{-diah})VO_2(hc)]$ (**1**–**3**), were synthesized in an acetonitrile/water mixture under aerobic conditions using H_2diah, $[VO(acac)_2]$, and the corresponding heterocycle (hc) in a 1:2:2 mol ratio in moderate yields. Here the oxygen in air acts as the oxidant for the oxidation of the metal centre from a +4 to +5 state. These yellow complexes are insoluble in common organic solvents except for dimethyl sulfoxide. The linear tetravanadium(IV,V,V,IV) complexes, $[(acac)_2OV(\mu\text{-O})VO(hc)(\mu\text{-diah})(hc)OV(\mu\text{-O})VO(acac)_2]$ (**4**–**6**), were synthesized by the same general procedure used for **1**–**3** using H_2diah, $[VO(acac)_2]$, and the corresponding heterocycle (hc) in a 1:4:2 mol ratio. Thus the twofold increase of the metal ion starting material, $[VO(acac)_2]$, results in the attachment of the excess amount at the two ends of **1**–**3** and hence the formation of two coordinatively unsymmetrical $\{OV(\mu\text{-O})VO\}^{3+}$ motifs in **4**–**6**. These complexes are green in colour and like **1**–**3** they are also soluble only in dimethyl sulfoxide. Electronic spectroscopic measurements indicate the formation of the tetravanadium species (**4**–**6**) in solution by the addition of 2 equiv. of $[VO(acac)_2]$ to yellow dimethyl sulfoxide solutions of the divanadium(V) complexes (**1**–**3**). The microanalysis data are consistent with the molecular formula of the complexes. In dimethyl sulfoxide, all the complexes are electrically nonconducting. The divanadium(V) complexes are diamagnetic, while the tetravanadium complexes are paramagnetic. The effective magnetic moments (μ_{eff}) of **4**–**6** at 298 K are within 2.31–2.37 μ_B. These values are consistent with the two unpaired electrons present at the two terminal vanadium(IV) centres of these complexes.

X-Ray Structures

The molecular structures of **1**, **3** and **6** are shown in Figures 1 and 2 and the bond parameters associated with the metal centres are listed in Tables 1 and 2. In each of the three structures, the two halves of the molecule are related by a crystallographically imposed inversion centre situated at the middle of the N–N bond of the dinucleating ligand $diah^{2-}$. The N=C [1.298(6)–1.308(4) Å] and the C–O [1.284(3)–1.292(6) Å] bond lengths in $diah^{2-}$ are consistent with the iminolate form [–N=C(O^-)–] of the amide functionalities.[2a–2g] The metal centres in **1** and **3** are in an O_3N_2 coordination sphere constituted by the imine-N and the amide-O of $diah^{2-}$, the imine-N of the heterocycle, and the two terminal oxido groups (Figure 1). In both complexes, the sum of the three O–V–O angles (359.9°) indicates that the metal atom is essentially at the centre of the O_3 triangular plane. The O–V–O angles are in the ranges 108.74(11)–130.78(9)° and 109.45(13)–132.29(11)° in **1** and **3**, respectively. The N1–V–N2 angle in **1** is 155.75(9)° and that in **3** is 154.09(9)°. These values may indicate that the geometry of the O_3N_2 coordination sphere is close to trigonal-bipyramidal, where the three O atoms form the trigonal plane and the two N atoms occupy the axial positions. For a better understanding of the nature of coordination geometry we have calculated the τ value[5] for both **1** and **3**. The τ is defined as $(\beta - \alpha)/60$, where β is the larger and α is the smaller *trans* bond angle in the basal plane. For ideal square-pyramidal and trigonal-bipyramidal geometries the τ will be zero and unity, respectively. Considering the bond angles (Table 1), a distorted square-pyramidal geometry can be thought of in each case, where the N1, N2, O′ and O3 form the basal plane and the O2 atom occupies the apical position. The τ values obtained are 0.42 and 0.36 for **1** and **3**, respectively. Thus the metal centres in both complexes are in a coordination geometry that is intermediate between trigonal-bipyramidal and square-pyramidal and is a little closer to the latter. The V–N(imine) and the V–O(amide) bond lengths are similar to the corresponding bond lengths observed in vanadium(V) complexes having the same coordinating atoms.[2] The V–N(heterocycle) bond lengths in **1** and **3** are significantly shorter than the corresponding bond

 © 2009 Wiley-VCH Verlag GmbH & Co. KGaA, Weinheim

lengths reported for vanadium(IV) complexes.[6] The V=O bond lengths are unexceptional when compared with the same in pentavalent vanadium complexes.[2–4] The V1···V1′ distances are 4.9292(8) and 4.953(2) Å in **1** and **3**, respectively. The V1···V1′ distance [4.946(2) Å] in **6** is very similar to that in **3**. Except for the V1–O2 bond length, the remaining bond parameters in this central dinuclear fragment of **6** (Figure 2) are also similar to the corresponding bond parameters found in complex **3**. As in **1** and **3** the O_3N_2 coordination sphere around each pentavalent vanadium centre (V1 and V1′) of **6** is slightly more towards square-pyramidal than trigonal-bipyramidal (τ = 0.39). The lengthening of V1–O2 in **6** is due to its coordination to the metal centre of the terminal $[VO(acac)_2]$ unit at the *trans* position with respect to its oxido atom O(8). The V2–O2 bond length is 2.418(4) Å. As a consequence of this coordination, the V–O(acetylacetonate) bond lengths [1.977(4)–1.986(4) Å] of the terminal distorted octahedral vanadium(IV) centres of **6** are marginally longer than those [1.967(1)–1.970(1) Å] observed in the structure of $[VO(acac)_2]$ where the metal centre is in square-pyramidal geometry.[7] For the same reason the displacement of the vanadium(IV) centre from the O_4 square-plane formed by the two acetylacetonate ligands towards the terminal oxido group is significantly less [0.365(2) Å] in **6** than the displacement [0.5447(4) Å] observed in the structure of $[VO(acac)_2]$.[7] However, the V2=O8 bond length [1.585(4) Å] is very similar to that [1.584(2) Å] of isolated $[VO(acac)_2]$.[7] The V1···V2 distance and the V1–O2–V2 bridge angle in the $\{OV(\mu\text{-}O)VO\}^{3+}$ cores of **6** are 3.951(1) Å and 154.0(2)°, respectively.

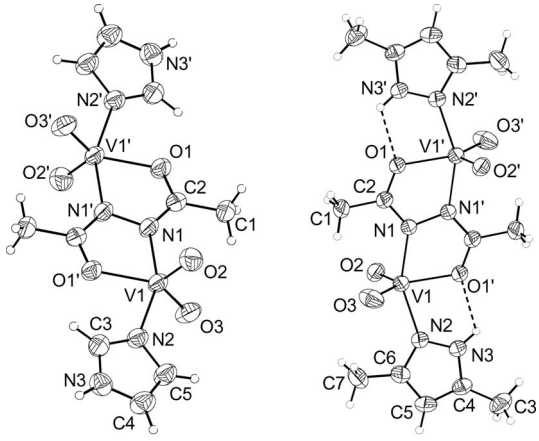

Figure 1. Molecular structures of (a) $[(Himdz)O_2V(\mu\text{-}diah)VO_2(Himdz)]$ (**1**) and (b) $[(Hdmpyz)O_2V(\mu\text{-}diah)VO_2(Hdmpyz)]$ (**3**) with the atom numbering schemes. All non-hydrogen atoms are represented by their 50% probability thermal ellipsoids.

The configuration of the mixed-valent $\{OV(\mu\text{-}O)VO\}^{3+}$ core has been found to be very important with respect to its electronic structure.[3g,3l] So far three configurations, namely *anti*-linear, *anti*-bent and *syn*-bent, have been detected in structurally characterized complexes of this core.[2h,3,4] Here "*anti*" or "s*yn*" refers to the relative orientation of the two terminal oxido groups in the {O=V(μ-O)-

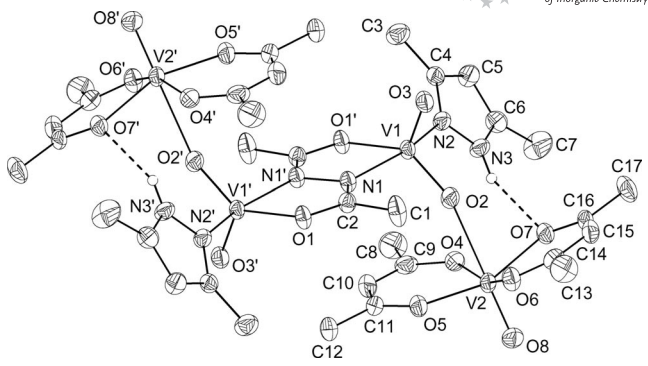

Figure 2. Molecular structure of $[(acac)_2OV(\mu\text{-}O)VO(Hdmpyz)(\mu\text{-}diah)(Hdmpyz)OV(\mu\text{-}O)VO(acac)_2]$ (**6**) with the atom numbering scheme. All non-hydrogen atoms are represented by their 30% probability thermal ellipsoids. All hydrogen atoms except for the NH hydrogen atom are omitted for clarity.

Table 1. Selected bond lengths [Å] and angles [°] for $\mathbf{1}\cdot 2H_2O$ and **3**.

Complex	$\mathbf{1}\cdot 2H_2O$[a]	**3**[b]
V1–N1	2.0751(19)	2.082(2)
V1–N2	2.070(2)	2.089(3)
V1–O2	1.6172(19)	1.622(2)
V1–O3	1.6152(18)	1.607(2)
V1–O1′	1.9921(17)	2.0165(19)
N1–V1–N2	155.75(9)	154.09(9)
N1–V1–O2	98.12(9)	99.16(10)
N1–V1–O3	97.18(9)	95.78(11)
N1–V1–O1′	74.70(7)	74.17(8)
N2–V1–O2	98.14(9)	99.16(10)
N2–V1–O3	94.47(9)	95.22(11)
N2–V1–O1′	81.58(7)	81.08(8)
O2–V1–O3	108.74(11)	109.45(13)
O2–V1–O1′	120.42(9)	118.12(11)
O3–V1–O1′	130.78(9)	132.29(11)

[a] Symmetry transformations used to generate equivalent atoms: $-x + 1, -y, -z$. [b] $-x, -y + 1, -z + 1$.

Table 2. Selected bond lengths [Å] and angles [°] for **6**.[a]

V1–N1	2.088(4)	V1–N2	2.090(4)
V1–O2	1.632(4)	V1–O3	1.589(4)
V1–O1′	1.990(3)		
V2–O2	2.418(4)	V2–O4	1.986(4)
V2–O5	1.977(4)	V2–O6	1.979(4)
V2–O7	1.983(3)	V2–O8	1.585(4)
N1–V1–N2	156.30(16)	N1–V1–O2	97.34(16)
N1–V1–O3	98.73(17)	N1–V1–O1′	74.35(14)
N2–V1–O2	94.05(16)	N2–V1–O3	97.02(18)
N2–V1–O1′	82.66(15)	O2–V1–O3	109.18(19)
O2–V1–O1′	132.91(18)	O3–V1–O1′	117.86(17)
O2–V2–O4	77.97(14)	O2–V2–O5	80.08(14)
O2–V2–O6	81.39(15)	O2–V2–O7	78.11(13)
O2–V2–O8	178.41(17)	O4–V2–O5	90.00(15)
O4–V2–O6	159.34(16)	O4–V2–O7	85.47(15)
O4–V2–O8	100.51(18)	O5–V2–O6	87.40(16)
O5–V2–O7	158.19(15)	O5–V2–O8	100.46(18)
O6–V2–O7	89.36(15)	O6–V2–O8	100.12(18)
O7–V2–O8	101.34(17)		

[a] Symmetry transformation used to generate equivalent atoms: $-x, -y + 1, -z + 1$.

 © 2009 Wiley-VCH Verlag GmbH & Co. KGaA, Weinheim

V=O}$^{3+}$ unit and "linear" or "bent" refers to the V–O–V angle. For ideal *anti* and *syn* configurations the O=V···V=O torsion angles are 180 and 0°, respectively. There is a single example of a configuration that is in between *syn*- and *anti*-bent.[3h] Here the O=V···V=O torsion angle is 83.7°. Such a configuration is also called "twist-angular".[3l] In all these species, the two (bridging)O–V=O angles are similar and less than 180°. The same is true for the two V···V=O angles. Interestingly, the bent {OV(μ-O)VO}$^{3+}$ cores in **6** are very different with respect to these angles. The O2–V1–O3 angle is 109.18(19)°, but the O2–V2–O8 angle is 178.41(17)°. The V2···V1–O3 and V1···V2–O8 angles are 124.6(1) and 168.4(2)°, respectively. These variations in the two halves of the {OV(μ-O)VO}$^{3+}$ core are primarily due to the differences in the coordination geometries around the V1 (intermediate between trigonal-bipyramidal and square-pyramidal) and V2 (distorted octahedral) and the *trans* relationship between the bridging and the terminal oxido groups at the V2. However, in relation to only the O3–V1···V2–O8 torsion angle [–166.2(7)°], the {OV(μ-O)VO}$^{3+}$ cores in **6** fall in the *trans*-bent category. So far the largest V···V distance reported is 3.7921(7) Å for a divanadium(V) species containing an unsymmetrical "twist angular" {OV(μ-O)-VO} core.[8] Possibly the unusually large V1···V2 distance [3.951(1) Å] in **6** is due to the atypical configuration of the {OV(μ-O)VO}$^{3+}$ core. Interestingly the V···V distance [3.3084(6) Å] in an unsymmetrical complex of {OV(μ-O)-VO}$^{4+}$ unit where one metal centre is square-pyramidal and the other one is distorted octahedral with a configuration very close to that observed in **6** is significantly smaller.[8]

Hydrogen Bonding and Self-Assembly

We have scrutinized all three structures for possible N–H···O type hydrogen bonding interactions as these complex molecules contain the heterocycle N–H group and fairly basic vanadium(IV/V)-bound oxido groups as well as metal-coordinated O atoms. Two water molecules are also present in the unit cell of **1**, which can participate in hydrogen-bonding interactions as a donor and as an acceptor.

In the case of **1**·2H_2O, the Himdz N–H group participates in an intermolecular N–H···O hydrogen bond involving the O4 atom of the lattice water as acceptor. The N3···O4 distance and the N3–H···O4 angle are 2.786(3) Å and 170°, respectively. The lattice water itself acts as a donor in two intermolecular O–H···O hydrogen bonds involving the two metal-coordinated oxido groups O2 and O3 as acceptors. The O4···O2 and O4···O3 distances are 2.846(3) and 2.871(3) Å, respectively. The O4–H···O2 and O4–H···O3 angles are 173(5) and 174(4)°, respectively. Because of these three intermolecular hydrogen-bonding interactions, **1**·2H_2O units assemble into a two-dimensional sheet structure (Figure 3). There is no other significant interaction between these parallel layers in the crystal lattice.

The Hdmpyz N–H group of **3** is involved in an intermolecular hydrogen-bonding interaction with one of the metal-bound oxido group O2. Here, the N3···O2 distance and the N3–H···O2 angle are 2.979(4) Å and 140°, respectively. Because of this N–H···O interaction the molecules of **3** forms a one-dimensional chain-like structure in the crystal lattice (Figure 3). The N–H group is also close to the metal-coordinated amide O1′ atom. The N3···O1′ distance and the N3–H···O1′ angle are 2.701(3) Å and 112°, respectively (Figure 1). These parameters perhaps indicate the involvement of the N–H group in bifurcated hydrogen bonds of inter- and intramolecular types.

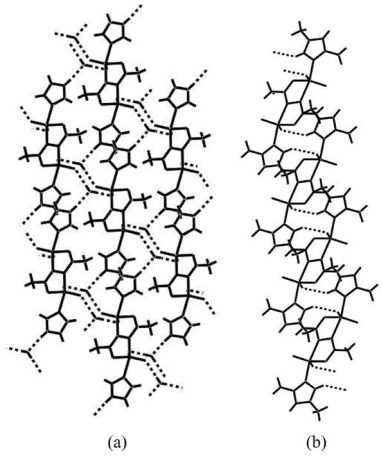

Figure 3. (a) Two-dimensional network of **1**·2H_2O and (b) one-dimensional chain structure of **3**.

In the case of **6**, there is no intermolecular hydrogen bonding and hence the molecules exist as discrete units in the crystal lattice. However, the Hdmpyz N–H group participates in an intramolecular N–H···O hydrogen bond involving one of the metal-coordinated acetylacetonate O atoms (Figure 2). The N3···O7 distance and the N3–H···O7 angle are 3.114(6) Å and 153°, respectively. Interestingly, this hydrogen bond indicates that there is a difference in the orientation of the Hdmpyz ring in the central dinuclear unit of **6** when compared with the isolated dinuclear species **3** where the N–H group is near the amide O1 atom (Figure 1). An approximately 180° rotation of the Hdmpyz ring along the V1–N2 will take away the N–H group from the amide O1 atom and bring it near the acetylacetonate O7 atom coordinated to the terminal metal centre V2 (Figure 2).

Spectroscopic Characteristics

The infrared spectra of **1**–**6** display a strong band in the range 1564–1545 cm^{-1}. This band is assigned to the C=N stretch of the dinucleating ligand diah^{2-}. A strong and a moderately strong band are observed in the ranges 959–932 and 898–850 cm^{-1} in the spectra of complexes **1**–**3**. These are attributed to the γ_{as} and γ_s stretches of the VO_2^+ unit.[2c–2e] Complexes **4**–**6** display a pair of strong bands in the 995–959 and 936–900 cm^{-1} regions due to the V^V=O and V^{IV}=O stretches, respectively.

 © 2009 Wiley-VCH Verlag GmbH & Co. KGaA, Weinheim

Electronic spectral profiles of **1**–**3** in dimethyl sulfoxide are very similar (Table 3). The spectra display two strong absorptions at about 308 and 275 nm due to ligand-to-metal and ligand-centred transitions.[3j–3l,8] Complexes **4**–**6** display two similar strong absorptions at about 313 and 274 nm. In addition to these two absorptions, they also display two weak absorptions in the ranges 575–550 and 415–423 nm (Table 3). Considering the trapped valence character of **4**–**6** in solution at room temperature (vide infra), it is very unlikely that any of these weak absorptions is due to intervalence transition.[2h,8] The electronic spectrum of $[VO(acac)_2]$ in dimethyl sulfoxide displays three absorptions at 650 (ε = 330 $M^{-1}cm^{-1}$), 453 (ε = 73 $M^{-1}cm^{-1}$) and 280 nm (ε = 875 $M^{-1}cm^{-1}$). Thus the weak absorptions observed in the visible region for **4**–**6** are assigned to the d–d transitions associated with the terminal vanadium(IV) centres.[3j–3l,8]

Table 3. Electronic spectroscopic[a] and cyclic voltammetric[a,b] data.

Complex	λ_{max} [nm] ($10^{-3}\times\varepsilon$ [$M^{-1}cm^{-1}$])	$E_{1/2}$[c] [V] (ΔE_p[d] [mV]) Reduction	Oxidation
1·$2H_2O$	308 (6.7), 270 (6.3)	–0.94[e]	–
2	309 (9.3), 277 (6.3)	–0.81 (380)	–
3	306 (11.4), 271 (6.4)	–0.78 (260)	–
4	560[f] (0.05), 420[f] (0.09), 312 (20.9), 273[f] (16.8)	–0.90[e]	0.96 (260)
5	575[f] (0.03), 415[f] (0.22), 313 (21.5), 273[f] (15.5)	–0.86[e]	0.99 (290)
6	550[f] (0.12), 423[f] (0.23), 313 (21.2), 275[f] (17.3)	–0.82[e]	1.12[g]

[a] In dimethyl sulfoxide (298 K). [b] At a scan rate of 100 mV s^{-1}. [c] $E_{1/2} = (E_{pa} + E_{pc})/2$, where E_{pa} and E_{pc} are anodic and cathodic peak potentials, respectively. [d] $\Delta E_p = E_{pa} - E_{pc}$. [e] E_{pc}. [f] Shoulder. [g] E_{pa}.

The ^1H NMR spectra of **1**–**3** have been recorded in $(CD_3)_2SO$. All the spectra display a singlet corresponding to three protons at δ = 2.50–2.52 ppm. This resonance is assigned to the methyl group of the dinucleating ligand $diah^{2-}$. The heterocycle NH proton appears as a broad singlet in the range 12.03–13.15 ppm. In the case of **1**, the three imidazole CH protons are observed as singlets at δ = 6.25, 7.60 and 8.18 ppm. Three singlets observed at δ = 6.26, 7.59 and 9.68 ppm for **2** are assigned to the three CH protons of the pyrazole ring. The 3- and 5-methyl protons of the Hdmpyz of **3** are observed as two singlets at δ = 2.27 and 2.11 ppm, respectively. The lone CH proton of the Hdmpyz resonates as a singlet at δ = 5.73 ppm. The ^{51}V NMR spectra of all three complexes display a singlet in the region δ = –516 to –542 ppm. These chemical shifts are comparable with the chemical shifts observed for similar dioxidovanadium(V) complexes.[9]

As expected, the diamagnetic dinuclear complexes **1**–**3** are EPR inactive. The paramagnetic tetranuclear complexes **4**–**6** in dimethyl sulfoxide at room temperature (298 K) display a clear eight-line ^{51}V (I = 7/2) hyperfine structure due to the terminal vanadium(IV) centres. The g_{iso} and A_{iso} values are within 1.97–1.98 and (94–97)$\times 10^{-4}$ cm^{-1}, respectively. In frozen (120 K) solution, all three complexes display typical well resolved axial spectra ($g_\parallel$ = 1.95–1.96, $A_\parallel$ = 166–173$\times 10^{-4}$ cm^{-1} and $g_\perp$ = 1.97–1.98, $A_\perp$ = 57–63$\times 10^{-4}$ cm^{-1}). Representative room temperature and frozen solution spectra are depicted in Figure 4. Observation of the room-temperature eight-line solution spectra instead of the 15-line spectra indicates the very rare solution phase localized electronic structure of the $\{OV(\mu\text{-}O)VO\}^{3+}$ cores in **4**–**6**.[2h,3g,3i,3l] Thus in fluid condition the valence delocalization commonly observed for mixed-valence $\{OV(\mu\text{-}O)VO\}^{3+}$ species is not favoured in **4**–**6** because of the very different coordination environment around the vanadium(IV) and vanadium(V) centres.

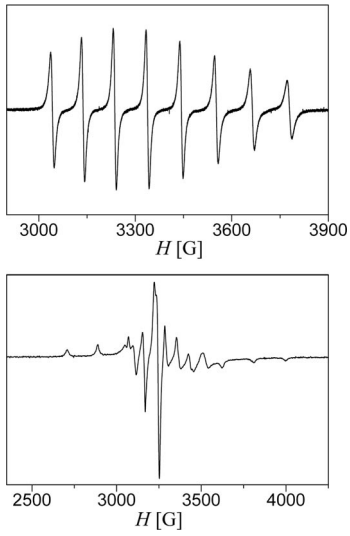

Figure 4. X-band EPR spectra of $[(acac)_2OV(\mu\text{-}O)VO(Hdmpyz)(\mu\text{-}diah)(Hdmpyz)OV(\mu\text{-}O)VO(acac)_2]$ (**6**) in dimethyl sulfoxide at 298 K (top) and 120 K (bottom).

Electrochemical Properties

Electron-transfer properties of **1**–**6** in dimethyl sulfoxide have been investigated with the help of cyclic voltammetry. The potential data have been listed in Table 3 and representative cyclic voltammograms are shown in Figure 5. The divanadium(V) complexes **1**–**3** display a reduction in the potential range –0.78 to –0.94 V (vs. Ag/AgCl). On the other hand, the tetravanadium(IV,V,V,IV) complexes (**4**–**6**) display a reduction as well as an oxidation in the potential ranges –0.82 to –0.90 V and 0.96 to 1.12 V (vs. Ag/AgCl), respectively. All these responses are irreversible because of unequal anodic and cathodic peak currents and large ΔE_p or the complete absence of the E_{pa} or E_{pc} (Table 3, Figure 5). The deprotonated bridging ligand ($diah^{2-}$) and the heterocycles do not show any such redox response in the above potential range. Thus the reduction response observed for all the complexes is assigned to the vanadium(V) → vanadium(IV) process, while the oxidation response observed for only the tetravanadium species (**4**–**6**) is attributed to the terminal vanadium(IV) → vanadium(V) process. The

 © 2009 Wiley-VCH Verlag GmbH & Co. KGaA, Weinheim

one-electron nature of these responses has been validated by comparing the peak currents with known one-electron transfer processes under identical conditions.[2,10] It may be noted that the reduction potentials (E_{pc} values) of **4**–**6** are higher than the corresponding values of **1**–**3**. This anodic shift of the vanadium(V) → vanadium(IV) reduction is possibly the consequence of the weakening of the V^{V}=O bond in the central dinuclear unit of **4**–**6** because of the coordination of the oxido group to the terminal vanadium(IV) centre.

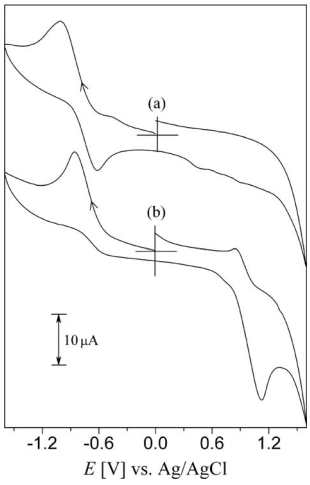

Figure 5. Cyclic voltammograms (scan rate 100 mV s^{-1}) of (a) [(Hpyz)O_2V(μ-diah)VO_2(Hpyz)] (**2**) and (b) [(acac)$_2$OV(μ-O)-VO(Hpyz)(μ-diah)(Hpyz)OV(μ-O)VO(acac)$_2$] (**5**) in dimethyl sulfoxide (0.1 M TBAP) at 298 K.

Conclusions

Dinuclear dioxidovanadium(V) complexes [(hc)O_2V(μ-diah)VO_2(hc)] **1**–**3** with O,N,N,O-donor *N*,*N*′-diacetyl hydrazine (H_2diah) and neutral N-donor heterocycles (hc) have been synthesized using [VO(acac)$_2$] as the metal ion source. In these complexes, the metal centres are in the trigonal-bipyramidal N_2O_3 coordination sphere. Use of double the amount of [VO(acac)$_2$] required for the synthesis of **1**–**3** provides linear tetravanadium(IV,V,V,IV) species [(acac)$_2$OV(μ-O)VO(hc)(μ-diah)(hc)OV(μ-O)VO(acac)$_2$] **4**–**6** containing two unsymmetrical $\{OV(\mu\text{-}O)VO\}^{3+}$ cores. X-ray structure of one of the tetravanadium species reveals that the mixed-valence core is in a trapped valence situation and it has a very unusual configuration with the largest V···V separation for this type of core.[8] Electronic spectra of **1**–**3** exhibit only ligand-to-metal charge transfer and ligand-based transitions in the UV region, while those of **4**–**6** show additional ligand field transitions in the visible region. The EPR results exhibit very rare valence localized electronic structures for **4**–**6** in the fluid matrix. All complexes are redox active. The divanadium(V) species display a vanadium(V) to vanadium(IV) reduction, while the tetravanadium(IV,V,V,IV) species display an additional vanadium(IV) to vanadium(V) oxidation with the metal-centred reduction.

Experimental Section

Materials: Bis(acetylacetonato)oxidovanadium(IV), [VO(acac)$_2$], was prepared by following a reported procedure.[11] All other chemicals and solvents used in this work were of analytical grade available commercially and were used without further purification.

Physical Measurements: Elemental (C, H, N) analysis data were obtained with the help of a Thermo Finnigan Flash EA1112 series elemental analyzer. Solution electrical conductivities were measured using a Digisun DI-909 conductivity meter. Magnetic susceptibility measurements were performed with a Sherwood Scientific balance. Diamagnetic corrections calculated from Pascal's constants[12] were used to obtain the molar paramagnetic susceptibilities. Infrared spectra were collected by using KBr pellets on a Jasco-5300 FTIR spectrophotometer. A Cary 100 Bio UV/Vis spectrophotometer was used to record the electronic spectra. The ^{1}H [Si(CH$_3$)$_4$ as internal standard] and ^{51}V ($VOCl_3$ as external standard) NMR spectra were collected with the help of Bruker 200 MHz and 400 MHz NMR spectrometers, respectively. A CH-Instruments model 620A electrochemical analyzer was used for cyclic voltammetric measurements with dimethyl sulfoxide solutions of the complexes containing tetrabutylammonium perchlorate (TBAP) as the supporting electrolyte. The three-electrode measurements were carried out at 298 K under dinitrogen with a glassy carbon working electrode, a platinum wire auxiliary electrode and an Ag/AgCl reference electrode. Under identical conditions the Fc^+/Fc couple was observed at 0.65 V. The potentials reported in this work are uncorrected for junction contributions.

Synthesis of the Complexes

[(Himdz)O_2V(μ-diah)VO_2(Himdz)]·2H_2O (1·2H_2O): An aqueous solution (5 mL) of *N*,*N*′-bis(diacetyl)hydrazine (116 mg, 1.0 mmol) was added to an acetonitrile solution (25 mL) of imidazole (136 mg, 2 mmol) and [VO(acac)$_2$] (530 mg, 2 mmol) and the mixture was boiled under reflux for 6 h and then filtered. The clear light yellow filtrate thus obtained was kept at 5 °C. A yellow crystalline complex started separating after about 3–4 d. The mixture was allowed to stay at low temperature for about 7 d to obtain the maximum yield and then the deposited crystalline material was collected by filtration washed with acetonitrile and dried in air; yield 185 mg (41%). $C_{10}H_{18}N_6O_8V_2$ (452.18): calcd. C 26.56, H 4.01, N 18.59; found C 26.37, H 4.18, N 18.42. ^{1}H NMR in (CD$_3$)$_2$SO: δ = 2.50 (s, CH$_3$), 6.25, 7.60, 8.18 (s, s, s, Himdz C-H protons), 13.15 (br. s, N-H) ppm. ^{51}V NMR in (CD$_3$)$_2$SO: δ = –542 (s) ppm.

[(Hpyz)O_2V(μ-diah)VO_2(Hpyz)] (2): This complex was synthesized in 48% yield by following an identical procedure as described for **1**·2H_2O except for the heterocycle being pyrazole instead of imidazole. $C_{10}H_{14}N_6O_6V_2$ (416.14): calcd. C 28.86, H 3.39, N 20.19; found C 28.54, H 3.17, N 19.83. ^{1}H NMR in (CD$_3$)$_2$SO: δ = 2.50 (s, CH$_3$), 6.26, 7.59, 9.68 (s, s, s, Hpyz C-H protons), 12.71 (br. s, N-H) ppm. ^{51}V NMR in (CD$_3$)$_2$SO: δ = –536 (s) ppm.

[(Hdmpyz)O_2V(μ-diah)VO_2(Hdmpyz)] (3): Using 3,5-dimethylpyrazole as the heterocycle this complex was obtained in 47% yield by following the same procedure used for the previous two complexes. $C_{14}H_{22}N_6O_6V_2$ (472.26): calcd. C 35.61, H 4.70, N 17.80; found C 35.49, H 4.78, N 17.64. ^{1}H NMR in (CD$_3$)$_2$SO: δ = 2.11 (s, 5-CH$_3$ of Hdmpyz), 2.27 (s, 3-CH$_3$ of Hdmpyz), 2.52 (s, CH$_3$), 5.73 (s, Hdmpyz C-H proton), 12.03 (br. s, N-H) ppm. ^{51}V NMR in (CD$_3$)$_2$-SO: δ = –516 (s) ppm.

[(acac)$_2$OV(μ-O)VO(Himdz)(μ-diah)(Himdz)OV(μ-O)VO(acac)$_2$] (4): This complex was prepared in 31% yield by following an identical procedure as described for **1**·2H_2O using H_2diah, Himdz and

 © 2009 Wiley-VCH Verlag GmbH & Co. KGaA, Weinheim

[VO(acac)$_2$] in a 1:2:4 mol ratio. Here the green complex started to crystallize within 2–3 d and it was isolated after keeping the reaction mixture at 5 °C for about a week to obtain the best yield. $C_{30}H_{42}N_6O_{16}V_4$ (946.46): calcd. C 38.07, H 4.47, N 8.88; found C 37.94, H 4.49, N 8.69. At 298 K μ_{eff} [μ_B]: 2.37. X-band EPR in $(CH_3)_2SO$: g_{iso} = 1.98, $A_{iso} = 94 \times 10^{-4}$ cm^{-1} at 298 K; $g_{\|}$ = 1.96, $A_{\|} = 173 \times 10^{-4}$ cm^{-1} and $g_{\perp}$ = 1.98, $A_{\perp} = 63 \times 10^{-4}$ cm^{-1} at 120 K.

[(acac)$_2$OV(μ-O)VO(Hpyz)(μ-diah)(Hpyz)OV(μ-O)VO(acac)$_2$] (5): A procedure identical to that described for **4** was used to prepare this complex in 26% yield using pyrazole instead of imidazole. $C_{30}H_{42}N_6O_{16}V_4$ (946.46): calcd. C 38.07, H 4.47, N 8.88; found C 37.81, H 4.24, N 8.52. At 298 K $\mu_{eff.}$ [μ_B]: 2.31. X-band EPR in $(CH_3)_2SO$: g_{iso} = 1.97, $A_{iso} = 96 \times 10^{-4}$ cm^{-1} at 298 K; $g_{\|}$ = 1.95, $A_{\|} = 166 \times 10^{-4}$ cm^{-1} and $g_{\perp}$ = 1.97, $A_{\perp} = 57 \times 10^{-4}$ cm^{-1} at 120 K.

[(acac)$_2$OV(μ-O)VO(Hdmpyz)(μ-diah)(Hdmpyz)OV(μ-O)VO(acac)$_2$] (6): This complex was prepared in 32% yield using 3,5-dimethylpyrazole as the heterocycle and a procedure identical to that used for the previous two complexes. $C_{34}H_{50}N_6O_{16}V_4$ (1002.56): calcd. C 40.73, H 5.03, N 8.38; found C 40.49, H 5.15, N 8.16. At 298 K $\mu_{eff.}$ [μ_B]: 2.36. X-band EPR in $(CH_3)_2SO$: g_{iso} = 1.97, $A_{iso} = 97 \times 10^{-4}$ cm^{-1} at 298 K; $g_{\|}$ = 1.95, $A_{\|} = 169 \times 10^{-4}$ cm^{-1} and $g_{\perp}$ = 1.98, $A_{\perp} = 58 \times 10^{-4}$ cm^{-1} at 120 K.

X-Ray Crystallography: Single crystals of **1**·2H$_2$O, **3** and **6** were collected directly from the products obtained during their syntheses. For each crystal, a Bruker-Nonius SMART APEX CCD single-crystal diffractometer, equipped with a graphite monochromator and a Mo-K_α fine-focus sealed tube (λ = 0.71073 Å) operated at 2.0 kW was used to determine the unit cell parameters and to collect the intensity data. The detector was placed at a distance of 6.0 cm from the crystal. Data were collected at 298 K with a scan width of 0.3° in ω and an exposure time of 10 s/frame. The SMART software was used for data acquisition and the SAINT-Plus software was used for data extraction.[13] The absorption corrections were performed with the help of the SADABS program.[14] The structures were solved by direct methods and refined on F^2 by full-matrix least-squares procedures. In all the structures, the non-hydrogen atoms were refined using anisotropic thermal parameters. The water hydrogen atoms in **1**·2H$_2$O were located in a difference map and refined with U_{iso}(H) = 1.5U_{iso}(O). All other hydrogen atoms were included in the structure factor calculations at idealized positions by using a riding model. The SHELX-97 programs[15] available in the WinGX package[16] were used for structure solution and refinement. The ORTEX6a[17] and Platon[18] packages were used for molecular graphics. Selected crystal and refinement data are listed in Table 4.

Table 4. Crystallographic data for **1**·2H$_2$O, **3** and **6**.

Complex	**1**·2H$_2$O	**3**	**6**
Empirical formula	$C_{10}H_{18}N_6O_8V_2$	$C_{14}H_{22}N_6O_6V_2$	$C_{34}H_{50}N_6O_{16}V_4$
Formula mass [g mol^{-1}]	452.18	472.26	1002.56
Crystal system	triclinic	monoclinic	triclinic
Space group	$P\bar{1}$	$P2_1/c$	$P\bar{1}$
a [Å]	7.3716(9)	7.196(3)	7.5769(15)
b [Å]	7.4285(9)	18.252(8)	10.388(2)
c [Å]	9.0578(11)	8.082(4)	15.675(3)
α [°]	106.516(2)	90	76.922(4)
β [°]	96.129(2)	112.156(7)	76.429(4)
γ [°]	107.765(2)	90	72.404(4)
V [Å^3]	442.58(9)	983.1(8)	1127.1(4)
Z	1	2	1
μ [mm^{-1}]	1.108	0.994	0.875
Measured reflections	4645	9294	12878
Unique reflections	1744	2303	5130
Reflections $I \geq 2\sigma(I)$	1537	1508	3235
Parameters	125	130	278
R_1, wR_2 [$I \geq 2\sigma(I)$]	0.0358, 0.0929	0.0498, 0.1036	0.0724, 0.1689
R_1, wR_2 (all data)	0.0417, 0.0964	0.0875, 0.1146	0.1176, 0.1868
GOF on F^2	1.062	0.946	1.038
$\Delta\rho_{max}$, $\Delta\rho_{min}$ [e Å^{-3}]	0.379, –0.202	0.530, –0.326	0.670, –0.329

CCDC-737096 (for **1**·2H$_2$O), -737097 (for **3**) and -737098 (for **6**) contain the supplementary crystallographic data for this paper. These data can be obtained free of charge from The Cambridge Crystallographic Data Centre via www.ccdc.cam.ac.uk/data_request/cif.

Acknowledgments

Financial assistance received from the Department of Science and Technology (DST), New Delhi (Grant No. SR/S1/IC-10/2007) is gratefully acknowledged. A. S. thanks the Council of Scientific and Industrial Research, New Delhi for a research fellowship. X-ray structures were determined at the National Single Crystal Diffractometer Facility, School of Chemistry, University of Hyderabad (established by the DST). We thank the University Grants Commission, New Delhi for the facilities provided under the UPE and CAS programs.

[1] a) N. D. Chasteen (Ed.), *Vanadium in Biological Systems*, Kluwer, Dordrecht, **1990**; b) A. Butler, M. J. Clague, G. E. Meister, *Chem. Rev.* **1994**, *94*, 625; c) H. Sigel, A. Sigel (Eds.), *Metal Ions in Biological Systems: Vanadium and its Role in Life*, Marcel Dekker, New York, **1995**, vol. 31; d) C. Slebodnick, B. J. Hamestra, V. L. Pecoraro, *Struct. Bonding (Berlin)* **1997**, *89*, 51; e) E. M. Page, *Coord. Chem. Rev.* **1998**, *172*, 111; f) D. Rehder, *Coord. Chem. Rev.* **1999**, *182*, 297; g) K. H. Thompson, J. H. McNeill, C. Orvig, *Chem. Rev.* **1999**, *99*, 2561; h) K. H. Thompson, C. Orvig, *Coord. Chem. Rev.* **2001**, *219–221*, 1033; i) *Chemistry and Biological Chemistry of Vanadium*, T. Hirao (Ed.), *Coord. Chem. Rev.* **2003**, *237*, 1–286; j) D. C. Crans, J. J. Smee, E. Gaidamauskas, L. Yang, *Chem. Rev.* **2004**, *104*, 849; k) Z. Janas, P. Sobota, *Coord. Chem. Rev.* **2005**, *249*, 2144; l) T. Kiss, T. Jakusch, D. Hollender, Á. Dörnyei, É. A. Enyedy, J. C. Pessoa, H. Sakurai, A. Sanz-Medel, *Coord. Chem. Rev.* **2008**, *252*, 1153; m) D. Rehder, *Bioinorganic Vanadium Chemistry*, Wiley, Chichester, **2008**.

[2] a) N. R. Sangeetha, V. Kavita, S. Wocadlo, A. K. Powell, S. Pal, *J. Coord. Chem.* **2000**, *51*, 55; b) N. R. Sangeetha, S. Pal, *Bull. Chem. Soc. Jpn.* **2000**, *73*, 357; c) S. N. Pal, S. Pal, *J. Chem. Crystallogr.* **2000**, *30*, 329; d) S. N. Pal, S. Pal, *Acta Crystallogr., Sect. C* **2001**, *57*, 141; e) S. N. Pal, K. R. Radhika, S. Pal, *Z. Anorg. Allg. Chem.* **2001**, *627*, 1631; f) A. Sarkar, S. Pal, *Inorg. Chim. Acta* **2008**, *361*, 2296; g) A. Sarkar, S. Pal, *Inorg. Chim. Acta* **2009**, *362*, 3807; h) A. Sarkar, S. Pal, *Eur. J. Inorg. Chem.* **2009**, 622.

[3] a) M. Nishizawa, K. Hirotsu, S. Ooi, K. Saito, *J. Chem. Soc., Chem. Commun.* **1979**, 707; b) P. Blanc, C. Madic, J.-P. Launay, *Inorg. Chem.* **1982**, *21*, 2923; c) F. Babonneau, C. Sanchez, J. Livage, J.-P. Launay, M. Daoudi, Y. Jeannin, *Nouv. J. Chem.* **1982**, *6*, 353; d) A. Kojima, K. Okajaki, S. Ooi, K. Saito, *Inorg. Chem.* **1983**, *22*, 1168; e) J.-P. Launay, Y. Jeannin, M. Daoudi, *Inorg. Chem.* **1985**, *24*, 1052; f) J. C. Pessoa, J. A. L. Silva, A. L. Vieira, L. Vilas-Boas, P. O'Brien, P. Thornton, *J. Chem. Soc., Dalton Trans.* **1992**, 1745; g) D. Schultz, T. Weyhermüller, K. Weighardt, B. Nuber, *Inorg. Chim. Acta* **1995**, *40*, 217; h) S. Mondal, P. Ghosh, A. Chakravorty, *Inorg. Chem.* **1997**, *36*, 59; i) M. Mahroof-Tahir, A. D. Keramidas, R. B. Goldfarb, O. P. Anderson, M. M. Miller, D. C. Crans, *Inorg. Chem.* **1997**, *36*, 1657; j) S. K. Dutta, S. B. Kumar, S. Bhattacharyya, E. R. T. Tiekink, M. Chaudhury, *Inorg. Chem.* **1997**, *36*, 4954; k) R. A.

 © 2009 Wiley-VCH Verlag GmbH & Co. KGaA, Weinheim

Holwerda, B. R. Whittlesey, M. J. Nilges, *Inorg. Chem.* **1998**, *37*, 64; l) S. K. Dutta, S. Samanta, S. B. Kumar, O. H. Han, P. Burckel, A. A. Pinkerton, M. Chaudhury, *Inorg. Chem.* **1999**, *38*, 1982.
[4] a) H. Kumagai, S. Kawata, S. Kitagawa, K. Kanamori, K. Okamoto, *Chem. Lett.* **1997**, *26*, 249; b) A. Neves, L. M. Rossi, A. J. Bortoluzzi, A. S. Mangrich, W. Haase, O. R. Nascimento, *Inorg. Chem. Commun.* **2002**, *5*, 418; c) C. Drouza, A. D. Keramidas, *Inorg. Chem.* **2008**, *47*, 7211.
[5] A. W. Addison, T. N. Rao, J. Reedijk, J. van Rijn, G. C. Verschoor, *J. Chem. Soc., Dalton Trans.* **1984**, 1349.
[6] a) H. Yue, D. Zhang, Y. Chen, Z. Shi, S. Feng, *Inorg. Chem. Commun.* **2006**, *9*, 959; b) E. Kine-Hunt, K. Spartalian, M. DeRusha, C. M. Num, C. J. Carrano, *Inorg. Chem.* **1989**, *28*, 4392.
[7] E. Shuter, S. J. Rettig, C. Orvig, *Acta Crystallogr., Sect. C* **1995**, *51*, 12.
[8] P. B. Chatterjee, S. Bhattacharya, A. Audhya, K.-Y. Choi, A. Endo, M. Chaudhury, *Inorg. Chem.* **2008**, *47*, 4891.
[9] a) X. Li, M. S. Lah, V. L. Pecoraro, *Inorg. Chem.* **1988**, *27*, 4657; b) C. A. Root, J. D. Hoeschele, C. R. Cornman, J. W. Kampf, V. L. Pecoraro, *Inorg. Chem.* **1993**, *32*, 3855; c) A. G. J. Ligtenbarg, A. L. Spek, R. Hage, B. L. Feringa, *J. Chem. Soc., Dalton Trans.* **1999**, 659; d) M. R. Maurya, S. Khurana, C. Schulzke, D. Rehder, *Eur. J. Inorg. Chem.* **2001**, 779; e) A. Sarkar, S. Pal, *Polyhedron* **2007**, *26*, 1205.
[10] a) S. G. Sreerama, S. Pal, *Inorg. Chem.* **2005**, *44*, 6299; b) R. Raveendran, S. Pal, *Eur. J. Inorg. Chem.* **2008**, 5540.
[11] R. A. Rowe, M. M. Jones, *Inorg. Synth.* **1957**, *5*, 113.
[12] W. E. Hatfield, in: *Theory and Applications of Molecular Paramagnetism* (Eds.: E. A. Boudreaux, L. N. Mulay), Wiley, New York, **1976**, p. 491.
[13] *SMART* V5.630 *and SAINT-plus* V6.45, Bruker-Nonius Analytical X-ray Systems Inc., Madison, WI, USA, **2003**.
[14] G. M. Sheldrick, *SADABS Program for Area Detector Absorption Correction*, University of Göttingen, Göttingen, Germany, **1997**.
[15] G. M. Sheldrick, *SHELX-97 Programs for Crystal Structure Analysis*, University of Göttingen, Göttingen, Germany, **1997**.
[16] L. J. Farrugia, *J. Appl. Crystallogr.* **1999**, *32*, 837.
[17] P. McArdle, *J. Appl. Crystallogr.* **1995**, *28*, 65.
[18] A. L. Spek, *PLATON: A Multipurpose Crystallographic Tool*, Utrecht University, Utrecht, the Netherlands, **2002**.

Received: July 20, 2009
Published Online: October 29, 2009

 © 2009 Wiley-VCH Verlag GmbH & Co. KGaA, Weinheim